



AC Loss in the Superconducting Cables of the CERN Fast Cycled Magnet Prototype

F. Borgnolutti¹, L. Bottura¹, A. Nijhuis², C. Zhou², B. Liu², Y. Miyoshi², H.J.G. Krooshoop², D. Richter¹,
1 CERN, Geneva, Switzerland
2 University of Twente, The Netherlands

Abstract

Fast Cycled Superconducting Magnets (FCM's) are an option of interest for the long-term consolidation and upgrade plan of the LHC accelerator complex. The economical advantage of FCM's in the range of 2 T bore field, continuously cycled at 0.5 Hz repetition rate, depends critically on the AC loss property of strand and cable. In this paper we report the results of the AC loss measurements that we have performed both on strands and cables manufactured for the CERN FCM prototype program.





Superconductivity Centennial Conference

AC loss in the superconducting cables of the CERN Fast Cycled Magnet Prototype

F. Borgnolutti^a, L. Bottura^{a*}, A. Nijhuis^b, C. Zhou^b, B. Liu^b, Y. Miyoshi^b,
H.J.G. Krooshoop^b, D. Richter^a

^aCERN, Geneva, Switzerland

^bUniversity of Twente, The Netherlands

Abstract

Fast Cycled Superconducting Magnets (FCM's) are an option of interest for the long-term consolidation and upgrade plan of the LHC accelerator complex. The economical advantage of FCM's in the range of 2 T bore field, continuously cycled at 0.5 Hz repetition rate, depends critically on the AC loss property of strand and cable. In this paper we report the results of the AC loss measurements that we have performed both on strands and cables manufactured for the CERN FCM prototype program.

© 2011 Published by Elsevier Ltd. Selection and/or peer-review under responsibility of Horst Rogalla and Peter Kes.

Keywords: Accelerators; Magnetization; Superconducting cables; Superconducting magnets

1. Introduction

In the present and widespread demand for improved energy management, we are running a focused R&D program on a *Fast Cycled superconducting Magnet* (or FCM) to examine the saving potential of superconducting accelerator magnets in the range of 2 T bore field and below. The target application is fast cycled synchrotrons, e.g. the PS injector for the LHC, running continuously at 0.5 Hz repetition rate. The energy efficiency in a superconducting magnet depends mainly on the heat balance at the cryogenic temperature level. The FCM design, described elsewhere [1], has several features that should optimize performance in this respect. One of the most important contributions to the overall heat balance is the AC

* Corresponding author.

E-mail address: Luca.Bottura@cern.ch.

loss in the conductor. This is why particular attention has been given to the development of a low-loss conductor suitable for this range of application. The FCM conductor is a Cable-Around-Conduit Conductor (CACC) based on the design principle developed at the Nuklotron, in Dubna, and manufactured by BNG Zeitz [2]. In our previous work we have reported critical current and strand magnetization in slowly varying fields. In this paper we focus on further extensive measurement and analysis of AC loss, including both hysteresis and coupling loss in strands and cable, which will serve as the benchmark to forecast and analyze AC loss data from the magnet test planned in the coming months.

2. Experimental

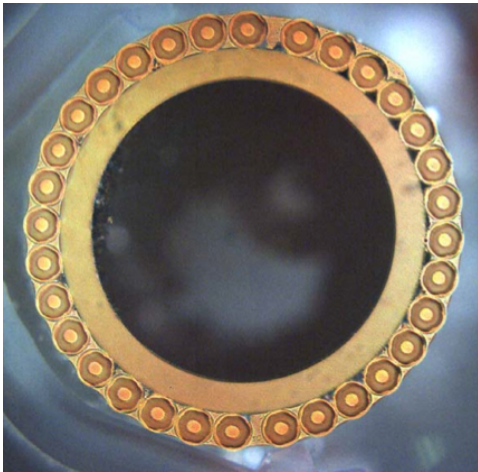


Fig. 1. Cross section of the FCM cable variant FCM001. The Ni-Cr wrap was removed and the strands were soldered only for the purpose of taking the micrography.

The FCM cable cross section is shown in Figure 1. The cable was produced in two variants that mainly differ for the Nb-Ti strands used. The first variant (FCM001) is based on an Alstom strand (46B01428) used for the inner layer of the LHC dipole. The strand was drawn from the original diameter of 1.025 mm, down to 0.6 mm to decrease the filament diameter D_f from 7 μm to 4 μm . The strand could be twisted with a relatively tight pitch of 6 mm. The second cable variant (FCM002) is based on a mixed matrix Cu/Cu-Mn/Nb-Ti strand (46B14040) that was produced by Alstom in the attempt to further decrease the filament diameter to 2.6 μm with minimal coupling among filaments. Due to manufacturing issues, the minimum achievable twist pitch of this strand was 10 mm, i.e. considerably higher than the practical lower limit of 10 times the strand diameter. Table 1 contains the main characteristics of the two strands. Note that for D_f we report the nominal geometric value (by design), while for critical current density J_C the values reported are based on the best measured performance. The strands are cabled around a

CuNi30Mn1 alloy tube with 5 mm inner diameter and 6 mm outer diameter, and kept in tight contact with the tube by a Ni-Cr8020 wire of 0.3 mm diameter. As can be seen in Fig. 1, the strands are in good contact with the Cu-Ni pipe, but the strand-strand contacts are not well defined (gaps can be observed at locations

Table 1. Main characteristics of the superconducting Nb-Ti strands used to manufacture the cables tested.

Strand ID	46B01428	46B14040
Diameter (mm)	0.6	
Twist pitch (mm)	6	10
Cu:Cu-Mn:Nb-Ti (-)	1.62:0:1	2.39:0.47:1
RRR (-)	58	110
D_f (μm)	4.1	2.6
$J_C(5T, 4.2 K)$ (A/mm^2)	2880	2015
n index (-)	50	25

Table 2. Main characteristics of the cable variants tested.

Cable ID	FCM001	FCM002
Strand ID	46B01428	46B14040
Strands (-)	32	33
Twist pitch (mm)	69.5	85.9
Outer diameter (mm)	7.74	
$I_C(5T, 4.2 K)$ (kA)	9.9	4.7

on the circumference). This is the result of the tolerance needed to accommodate the strands around the pipe circumference during the cabling process. It is a much desirable feature of the cable design, because it yields to a loose contact among strands, and relatively high effective adjacent inter-strand resistance R_a . As we will describe later, high values of R_a are useful to decrease coupling among strands and thus achieve the desired low AC loss. In Table 2 we report the main characteristics of the two cable variants.

2.1. Measurement set-up and samples

AC loss measurements were performed in a superconducting dipole providing a varying field transverse to the strand and the cable samples. The field range explored was up to 1.5 T, for frequencies from 0.01 Hz to 0.2 Hz. This data range was chosen to allow reliable extrapolation to the magnet operating conditions, i.e. peak field of 1 T and trapezoidal ramps at 0.5 Hz [1]. The loss was measured using both magnetization (using pick-up coils) and calorimetry (based on the boil-off massflow). All measurements reported here were taken in a liquid helium bath at atmospheric pressure, at 4.2 K. The test set-up and methods are described elsewhere [3]. Strand samples consisted of single layer coils with 40 mm diameter, wound with a total strand length of about 0.18 m. Cable samples consisted of bundles of 10 straight pieces, each piece being 420 mm long. The strands and cables were cut using a diamond wire saw that guarantees no smearing of the materials and avoids coupling at the sample ends. A particular of interest is that we impregnated the cable ends with epoxy in the portion where the cut took place, to secure the Ni-Cr wrap and thus maintain the contact pressure of the strands against the inner tube.

3. Strand AC loss

The strand AC loss is known to have two main components, hysteresis Q_h due to the persistent currents in the filaments and coupling of the filaments Q_c through the resistive matrix. To distinguish between the two components, we have performed measurements with sinusoidal and triangular field waveforms, at varying frequency. The hysteresis loss is the zero-frequency limit of the measured loss, obtained by

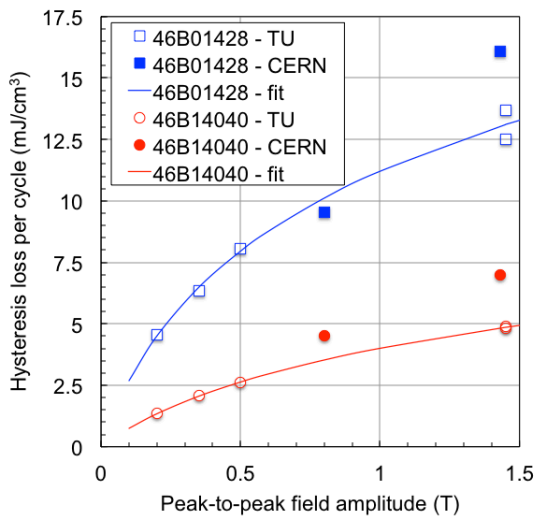


Fig. 2. Summary of hysteresis loss in the two strands variants.

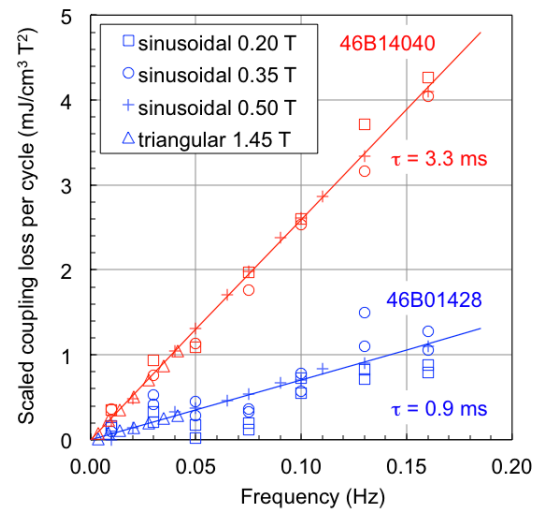


Fig. 3. Summary of coupling loss in the two strands variants, scaled by the square of the field change amplitude.

extrapolation of the measured data. The coupling loss is the frequency dependent component, obtained subtracting the hysteresis loss from the measured values. We report in Figs. 2 and 3 the main results of the strand measurements, summarized as a plot of hysteresis loss vs. the (peak-to-peak) amplitude of the field change B_a (Fig. 2), and a plot of scaled coupling loss vs. frequency f (Fig. 3).

The hysteresis loss shown in Fig. 2 is a compilation of all data collected. For unipolar cycles ($0 \Rightarrow B_a \Rightarrow 0$, with $B_a = 1.45$ T) we plot the measured value. In case of bipolar cycles ($-B_a \Rightarrow B_a \Rightarrow -B_a$ with B_a in the range of 0.2 to 0.5 T), we report half of the value measured. This corresponds to making the hypothesis that the magnetization curve is symmetric and that the energy loss during partial penetration is negligible. The hysteresis loss for strand 46B14040 (mixed Cu/Cu-Mn matrix) is significantly smaller (a factor three) than for strand 46B01428 (Cu matrix). As discussed earlier [2], this is mainly due to the lower fraction of superconductor in the strand, and to the reduced J_C . Indeed, the effective filament diameter that can be deduced from the width of the magnetization loop is essentially the same in both strands, of the order of 4 μm . These results confirm the direct observation of micrographs of strand 46B14040, also reported in [2], where we postulated that the large deformation of the Nb-Ti filaments can justify the relatively large effective filament in spite of the de-coupling properties of the Cu-Mn matrix. The Q_h results for both strands can be fitted very well with a simple model derived integrating the magnetization of a fully penetrated filament and Kim-like critical current at low field:

$$Q_h = \frac{4}{3\pi} \lambda D_{\text{filament}} J_0 B_0 \ln \left(\frac{B_0 + B_a}{B_0} \right) \quad (1)$$

where λ is the superconductor fraction in the strand, and J_0 and B_0 are the fit constants. Their values for strand 46B01428 are $J_0 = 52.3$ kA/mm² and $B_0 = 0.17$ T, and $J_0 = 19.3$ kA/mm² and $B_0 = 0.35$ T for strand 46B14040. For completeness, we report in Fig. 2 the hysteresis loss quoted earlier [2] obtained using the CERN magnetometer [4]. We note that the measurement discussed here (marked as ‘‘TU’’ in Fig. 2) are systematically lower than those quoted earlier (marked as ‘‘CERN’’ in Fig. 2), by 20 % on average. Besides sample variability, the difference is not surprising and can be attributed to cross calibration issues to be resolved in the future. This difference can be taken as an indication of the uncertainty on the overall estimate discussed below.

The data for coupling loss in Fig. 3 also combines measurements in different conditions. Data from sinusoidal excitation is scaled by the square of the amplitude of the field change B_a^2 and plotted vs. frequency, while data from triangular cycles is scaled by an additional factor $\pi^2/8$, discussed later, and plotted vs. $1/T$ where T is the total time of a cycle. The scaled coupling loss has excellent linearity in the range of frequency examined, which is an evidence of low-frequency regime. An equivalent time constants can be derived fitting the measured loss with the low-frequency approximations:

$$\frac{Q_c}{B_a^2} = \frac{n\pi}{\mu_0} \begin{cases} \frac{4}{T} & \text{trapezoidal} \\ \frac{\pi^2}{2} f & \text{sinusoidal} \end{cases} \quad (2)$$

where n is the demagnetization factor, taken equal to 2. Note that the ratio of the scaled losses at the same frequency is equal to the normalization factor $\pi^2/8$ quoted earlier, which can be hence used to compare directly sinusoidal and triangular excitation. Consistency in the values of the two waveforms at a given frequency confirms that the low-frequency interpretation is correct.

The values of the time constants obtained are 0.9 ms for the strand 46B01428 (Cu matrix), and 3.3 ms for the strand 46B14040 (mixed Cu/Cu-Mn matrix). This result is within the range of estimates that can be obtained using simple theory in the limit of high contact resistance between filaments and matrix [5]. The fact that the Cu matrix strand 46B01428 has lower coupling than the mixed matrix strand 46B14040 is not surprising. Indeed, the advantage of the Cu-Mn resistive matrix (a factor 2 higher resistivity than pure Cu) is more than offset by the longer twist pitch of strand 46B14040 (nearly a factor 2), and the influence of large filaments deformation that reduces the effective transverse resistance of the matrix.

4. Cable AC loss

AC loss results in the two cable samples are reported in Figs. 4 and 5, using the same vertical scale for ease of comparison. Both cables show similar behaviors, i.e. a marginal increase of the strand loss due to coupling currents in the cable, and saturation at low frequency. Interestingly, and somewhat surprisingly, the saturation frequency *decreases* at *increasing* field amplitude. In fact, it is not possible to extract a simple linear dependency from the data reported there, as done for the strand coupling, nor is scaling with the square of the field change amplitude successful. A low frequency fit of the loss using Eq. (2) (the low frequency slope) yields to effective loss constant $n\tau$ of 18 ms for cable FCM001, and 10 ms for cable FCM002. This is however a largely pessimistic estimate. Indeed, examining the trend in the experimental data, it is expected that the contribution of cable coupling loss is very small at the design point for the field change amplitude (1 T) and frequency (0.5 Hz) in the magnet and, in practice, can be neglected.

To substantiate the above argument, a direct measurement of adjacent inter-strand resistance has yielded values in the range of 2.1 to 2.3 m Ω per mm of contact length, which is very high and consistent with the observation that strands do not have tight packing on the perimeter of the tube. We believe that the observed behavior is a signature of the relatively ill-defined inter-strand contact that results in a number of small coupling loops with low resistance that affect only a limited portion of the cable. Each loop has a long time constant, saturates at low frequency, and produces a small loss. Similar behavior has been observed in multi-stage cables such as those used in CICC's [6].

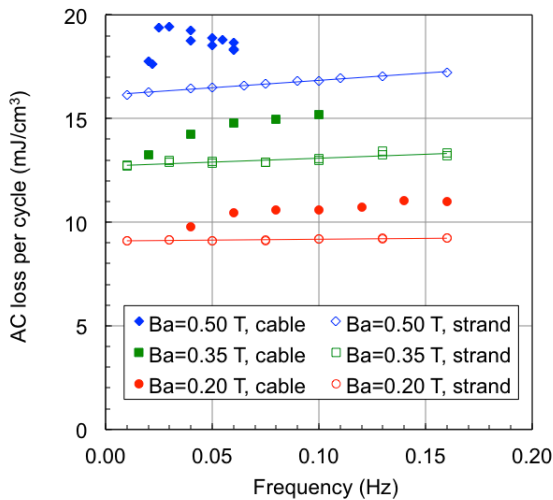


Fig. 4. AC loss per cycle in the cable FCM001 as a function of frequency for sinusoidal excitation at various field amplitudes.

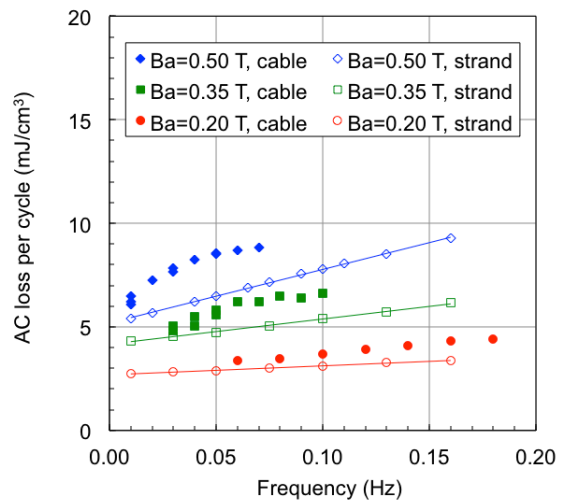


Fig. 5. AC loss per cycle in the cable FCM002 as a function of frequency for sinusoidal excitation at various field amplitudes.

5. Conclusions

The AC loss of the cable variants manufactured for the FCM prototype has been characterized in a regime of field amplitude and frequency of relevance for the prediction and interpretation of magnet test data. Known theory was found to describe very well the measured strand behavior, and allows precise extrapolation to the operating conditions of the FCM magnet. The cable coupling loss exhibits early saturation, and is small compared to the strand loss components, as desired. We believe that this is due to the relatively ill-defined network of contacts between adjacent strands, and in practice will have a negligible effect on the magnet performance.

Based on the measured properties, and taking the design operating point at 1 T field change and 0.5 Hz triangular excitation, we obtain a predicted loss per cycle and unit volume of strand of 10 mJ/cm^3 for the cable FCM001 (Cu matrix strand), of which $2/3$ are due to hysteresis and $1/3$ to coupling. In the case of cable FCM002 (mixed Cu/Cu-Mn strand), the predicted loss per cycle and unit strand volume is 13 mJ/cm^3 , of which hysteresis only accounts for $1/5$, while coupling represents $4/5$ of the total. Further loss reduction would hence be possible if the mixed matrix strand could be twisted with a shorter pitch. The two cables have AC loss well within the allocated thermal budget of the magnet prototype. Specifically, using the above values we expect approximately 1 W/m of magnet length at nominal operation, which represents 20 % of the total estimated heat load at 4.2 K and is an excellent result.

It is finally interesting to remark how the cable has negligible coupling, and high inter-strand resistance, but did not exhibit any visible ramp-rate dependence of the quench current, as discussed in [2]. We believe this is due to the precise transposition of the strands, arranged around a well-defined round geometry, resulting in little stray fluxes and current imbalance.

References

- [1] L. Bottura, et al., “Construction of the CERN Fast Cycled Superconducting Dipole Magnet Prototype,” Paper presented at MT-22, September 2011, Marseille, to appear in *IEEE Trans. Appl. Sup.* 2012.
- [2] L. Bottura, et al., “Strand and Cable R&D for Fast Cycled Magnets at CERN,” *IEEE Trans. Appl. Sup.*, 21, (2001) pp. 2354 – 2358.
- [3] A. Nijhuis, et al., “First results of a parametric study on coupling loss in sub-size NET/ITER Nb3Sn cabled specimens,” *IEEE Trans App Supercond* 5, (1995) pp. 992-995.
- [4] S. Le Naour, et al., “Test station for magnetization measurements on large quantities of superconducting strands,” *IEEE Trans. App. Sup.*, 11, (2001) pp 3086 – 3089.
- [5] M. Wilson, *Superconducting Magnets*, Clarendon Press, Oxford, 1983.
- [6] A. Nijhuis, et al., “Study on the coupling loss time constants in full size Nb3Sn CIC model conductors for fusion magnets (1995), *Adv Cryog Eng.*: 42B, pp.1281-1288.